Missense mutation in the *tubulin-specific chaperone E* (*Tbce*) gene in the mouse mutant *progressive motor neuronopathy,* a model of human motoneuron disease

Heike Bömmel,[1] Gang Xie,[1] Wilfried Rossoll,[1] Stefan Wiese,[1] Sibylle Jablonka,[1] Thomas Boehm,[2] and Michael Sendtner[1]

[1]Institute of Clinical Neurobiology, University of Würzburg, 97080 Würzburg, Germany
[2]Max-Planck-Institute for Immunobiology, 79108 Freiburg, Germany

Progressive motor neuronopathy (*pmn)* mutant mice have been widely used as a model for human motoneuron disease. Mice that are homozygous for the *pmn* gene defect appear healthy at birth but develop progressive motoneuron disease, resulting in severe skeletal muscle weakness and respiratory failure by postnatal week 3. The disease starts at the motor endplates, and then leads to axonal loss and finally to apoptosis of the corresponding cell bodies. We localized the genetic defect in *pmn* mice to a missense mutation in the *tubulin-specific chaperone E (Tbce)* gene on mouse chromosome 13. The human orthologue maps to chromosome 1q42.3. The *Tbce* gene encodes a protein (cofactor E) that is essential for the formation of primary α-tubulin and β-tubulin heterodimeric complexes. Isolated motoneurons from *pmn* mutant mice exhibit shorter axons and axonal swelling with irregularly structured β-tubulin and tau immunoreactivity. Thus, the *pmn* gene mutation provides the first genetic evidence that alterations in tubulin assembly lead to retrograde degeneration of motor axons, ultimately resulting in motoneuron cell death.

Introduction

Autosomal recessive traits of motoneuron disease are observed in classical spinal muscular atrophy (SMA;* Lefebvre et al., 1995), in SMA with respiratory distress type 1 (SMARD1; Grohmann et al., 2001), and in a rare form of juvenile amyotrophic lateral sclerosis (ALS2; Hadano et al., 2001; Yang et al., 2001). The responsible gene defects have been characterized; SMA and SMARD1 are caused by defects in RNA processing. The discovery of gene defects in ALSIN/ALS2, a GTPase with structural similarities to RanGEF as well as RhoGEF in ALS2 (Hadano et al., 2001; Yang et al., 2001), has given a first hint from human genetic studies that signaling mechanisms regulating cytoskeletal turnover might also be disturbed in motoneuron disease. Motoneurons differ from other types of neurons within the spinal cord by the length of their axons, which can reach a length of >1 m in adult human. Structural and functional maintenance of these large cells are dependent on the axonal transport of organelles and cytoskeletal proteins. Deficiency or interruption of axonal transport has been previously reported as a cause of motoneuron disease (Cote et al., 1993; Xu et al., 1993; LaMonte et al., 2002). However, in a significant number of SMA and sporadic ALS cases, the underlying gene defects have not yet been identified. Therefore, the characterization of additional disease genes is expected to provide further information on the pathophysiology of motoneuron disease.

The autosomal recessive *progressive motor neuronopathy* (*pmn*) mouse mutant (Schmalbruch et al., 1991*)* resembles SMA by progressive degeneration of motoneurons in the early postnatal period. Genetic mapping has identified the *pmn* locus on mouse chromosome 13 in a region defined by markers D13Mit172 and D13Mit207 (Martin et al., 2001). We localized the genetic defect to a point mutation in the *tubulin-specific chaperone E* (*Tbce*) gene affecting an evolu-

The online version of this article includes supplemental material.

Address correspondence to Michael Sendtner, Institute of Clinical Neurobiology, University of Würzburg, Josef-Schneider-Strasse 11, 97080 Würzburg, Germany. Tel.: 1149-931-201-49767. Fax: 1149-931-201-49788. E-mail: sendtner@mail.uni-wuerzburg.de

H. Bömmel and G. Xie contributed equally to this work.

G. Xie's present address is Mount Sinai Hospital, Samuel Lunenfeld Research Institute, Toronto, Canada.

*Abbreviations used in this paper: ALS, amyotrophic lateral sclerosis; BAC, bacterial artificial chromosome; CofE, cofactor E; *pmn*, *progressive motor neuronopathy*; SMA, spinal muscular atrophy; SMARD1, SMA with respiratory distress type 1; STS, sequence-tagged site; *Tbce*, *tubulin-specific chaperone E*; wt, wild type; YAC, yeast artificial chromosome.

Key words: *pmn*; motoneuron disease; tubulin; tubulin-specific chaperone E; motor axon

© The Rockefeller University Press, 0021-9525/2002/11/563/7 $5.00

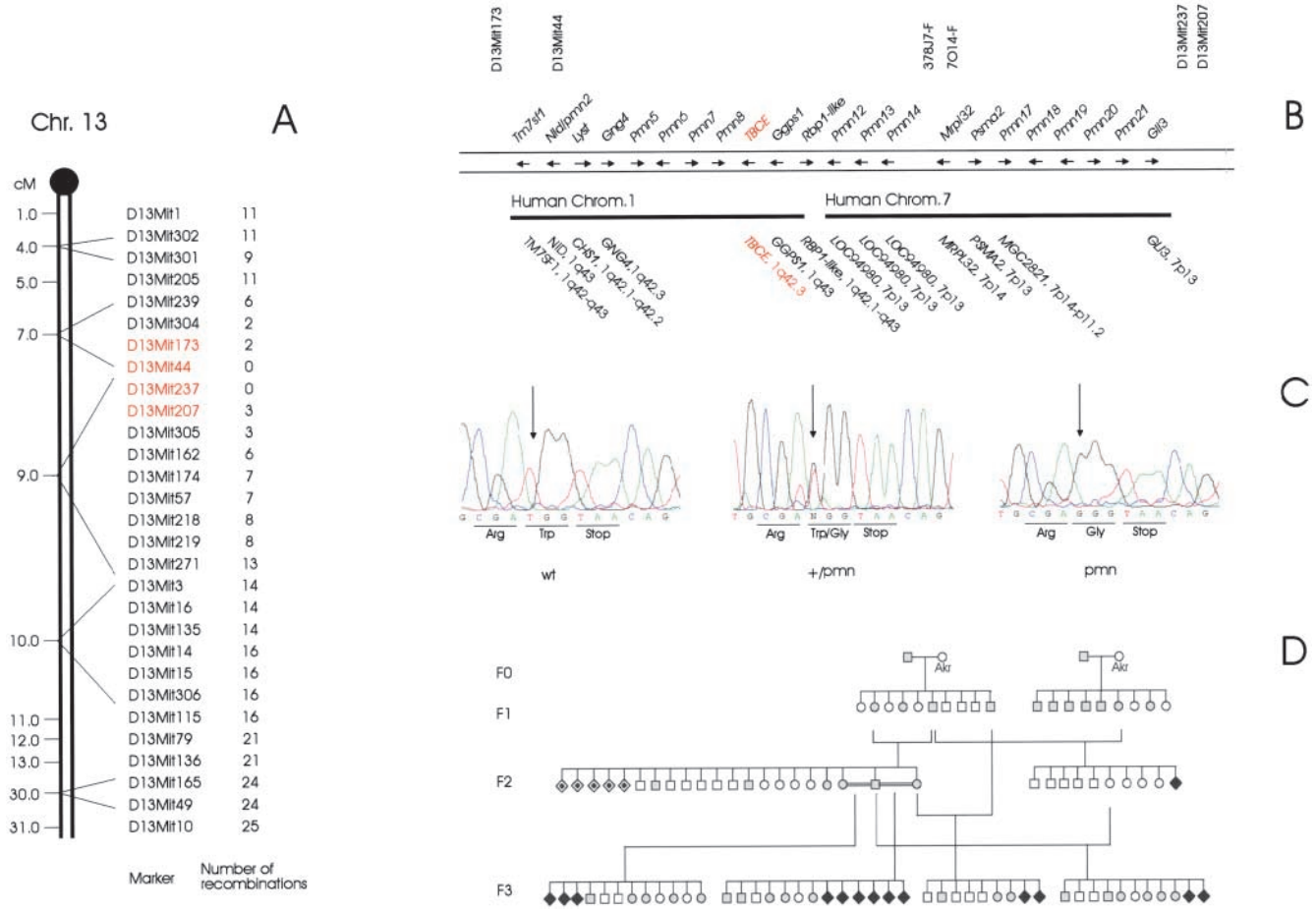

Figure 1. **Characterization of the gene defect in *pmn* mice.** (A) Genetic map of the *pmn* candidate region. (B) Transcript map of the *pmn* region including the synteny region of the human genome. Transcriptional units not present in public databases were numbered according to their succession in this region. *Pmn2* is located in noncoding regions of *Nid*. (C) Primary genomic DNA sequence of *Tbce* in *pmn,* heterozygous, and NMRI wt mice. Sequences of the sense strand are shown. The arrow indicates the T→G base mutation. The mutation leads to an exchange of the amino acid Trp to Gly. (D) Segregation of the homozygous $Tbce^{G}/Tbce^{G}$ mutation with the *pmn* disease phenotype. One representative pedigree is shown. Homozygous $Tbce^{G}/Tbce^{G}$ mutation was only found in *pmn* mice (black symbols). Healthy littermates were either heterozygous for the $Tbce^{G}$ mutation ($Tbce^{W}/Tbce^{G}$; gray symbols) or homozygous wt ($Tbce^{W}/Tbce^{W}$; white symbols). The animals marked with a black dot showed symptoms of motoneuron disease but died before genotyping was initiated.

tionary conserved amino acid residue. The identification of this gene defect may help to define new candidate genes that are mutated and thus might be involved in the pathophysiology underlying human motoneuron disease.

Results and discussion

To identify the corresponding gene defect in *pmn* mice, we have performed detailed genetic mapping by genotyping 229 *pmn/pmn* F2 progeny from one male NMRI founder that was heterozygous for the *pmn* gene defect and two female AKR mice. 29 microsatellite markers spanning a region of 31 cM were used and 34 recombination events were observed (Fig. 1 A). Our results refined the *pmn* locus to a 2-cM region flanked by markers D13Mit173 and D13Mit207.

We generated a yeast artificial chromosome (YAC)– and a bacterial artificial chromosome (BAC)–based physical map of the genomic region encompassing nearly the entire *pmn* candidate region (Fig. S1, available online at http://www.jcb.org/cgi/content/full/jcb.200208001/DC1). Sequences from the ends of YAC and BAC clones were subsequently integrated into the complete sequence of the region flanked by markers D13Mit173 and D13Mit207 when this information became available in public and Celera databases. The characterized region had a size of ~2.19 Mb. Together with previously published data (Martin et al., 2001), the critical region could be refined between D13Mit173 and 378J7-F, which is located between *Pmn14* and *Mrpl32* (Fig. 1 B; Table S1, available online at http://www.jcb.org/cgi/content/full/jcb.200208001/DC1).

Comparative analysis of mouse and human homology maps resulted in a transcript map of the *pmn* critical region (Fig. 1 B; Table S1). Synteny with segments located on human chromosomes 1q42–q43 and 7p14.1–p13 was found, as described earlier (Martin et al., 2001). We mapped 15 transcriptional units between D13Mit173 and 378J7-F and 23 between D13Mit173 and D13Mit237, including 11 previously characterized genes and 12 transcripts that all had been identified before as EST in mouse and human. cDNA

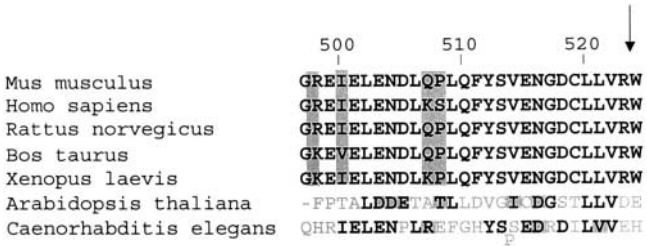

Figure 2. **Multiple amino acid sequence alignment of the COOH-terminal region of CofE from different vertebrate and nonvertebrate species.** The nucleotide sequences of CofE were taken from public databases, translated to the corresponding amino acid sequence, and then aligned using ExPasy (www2.ebi.ac.uk/clustal). The amino acid numbers correspond to murine CofE. Conserved substitutions and semiconserved substitutions are indicated in gray; the remaining black amino acids are identical. Amino acids without similarity are shown in light gray. The arrow indicates the amino acid mutated in *pmn* mice.

from brain of *pmn/pmn* and NMRI wild-type (wt) mice was sequenced for all 11 previously characterized genes and 12 new transcripts to identify the possible mutation. Among the 23 genes surveyed, only one gene was found to carry a specific change in sequence, which was subsequently confirmed by sequencing genomic DNA from *pmn* mice. A T→G transition occurred at nucleotide position 1682 of the *Tbce* gene (Fig. 1 C). This results in a missense mutation exchanging tryptophan for glycine at position 524 of the murine cofactor E (CofE) protein. Sequence comparison revealed that this amino acid is strictly conserved among vertebrate species (Fig. 2). In nonvertebrate orthologues such as *Arabidopsis thaliana* and *Caenorhabditis elegans*, glutamate and histidine are found instead of tryptophan at this position. It is not clear whether this alteration correlates with specific differences in chaperone function in tubulin assembly between vertebrate and nonvertebrate species. At least for the homologue of vertebrate cofactor A, such differences have been proposed from genetic studies with *Schizosaccharomyces pombe* (Radcliffe et al., 2000).

To correlate this mutation with the *pmn* phenotype, we analyzed 60 *pmn/pmn* and 147 wt mice. These mice were obtained from our breeding colony. They were not related to the heterozygous male used for the initial backcross with AKR. RT-PCR was performed with RNA from both the brain and spinal cord. In addition, genomic DNA was investigated to rule out that the nucleotide exchange is due to posttranscriptional mechanisms. This specific mutation in both alleles in the *Tbce* gene clearly co-segregated with the *pmn* disease phenotype. Healthy littermates were either heterozygous for the *Tbce* mutation or homozygous wt, according to Mendelian rules (Fig. 1 D). In addition, mice with NMRI, AKR, C57BL/6, or 129SvJ genetic background were screened. In none of these mice, the T→G transition in the *Tbce* gene was observed.

The protein encoded by the *Tbce* gene (CofE) plays an essential role as a tubulin-specific chaperone that binds to α-tubulin and thus helps in its assembly with β-tubulin (Tian et al., 1996). This specific function is conserved between species ranging from yeast (Hoyt et al., 1997; Radcliffe et al., 1999) to mammals (Tian et al., 1997). During translation, tubulin subunits are folded to a quasi-native state by the cytosolic chaperonin CCT (Hartl, 1996). The tubulin-specific chaperones, which include CofE, subsequently assemble the native tubulin heterodimer. Therefore, disturbances of this process are expected to result in altered formation of α- and β-tubulin heterodimers and should interfere with assembly of microtubules. To test this hypothesis, we isolated motoneurons from embryonic day 13.5 wt and *pmn* mutant mice. The identification of the genetic defect in *pmn* mice allowed us, for the first time, to genotype *pmn/pmn* mouse embryos at day 13.5 and to distinguish them from wt and heterozygous littermates. After a culture period of 7 d in the presence of 1 ng/ml BDNF, the motoneurons were fixed, stained with antibodies against tau and β III tubulin, and the length of axonal processes was measured by observers who were blinded with respect to the genotype. In *pmn* mutant motoneurons, both the length of the longest axon and the total length of the axon including all its branches (Fig. 3, A and B; Fig. 4, A and B) were significantly reduced, by 58.77 ± 1.25% and 64.76 ± 3.66%, respectively (mean ± SEM, three independent experiments from nine *pmn/pmn* and seven wt embryos).

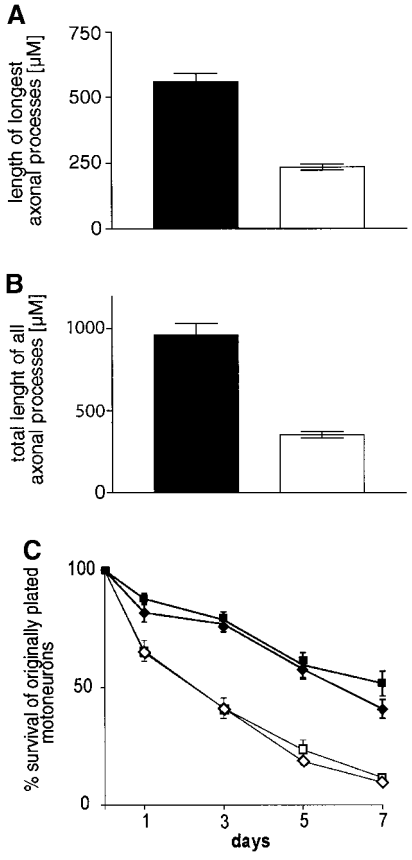

Figure 3. **Axonal growth and survival in isolated wt and *pmn* mutant motoneurons.** (A and B) After 7 d in culture with 1 ng/ml BDNF, the length of the longest axon and the total length of the axon including all its branches from *pmn* mutant motoneurons ($Tbce^G/Tbce^G$; open bar) are significantly ($P < 0.0001$) shorter than from wt motoneurons ($Tbce^W/Tbce^W$; closed bar). (C) Survival of motoneurons isolated from wt ($Tbce^W/Tbce^W$; ◆) and *pmn* mice ($Tbce^G/Tbce^G$; ■) in the presence (closed symbols) and absence (open symbol) of 1 ng/ml BDNF.

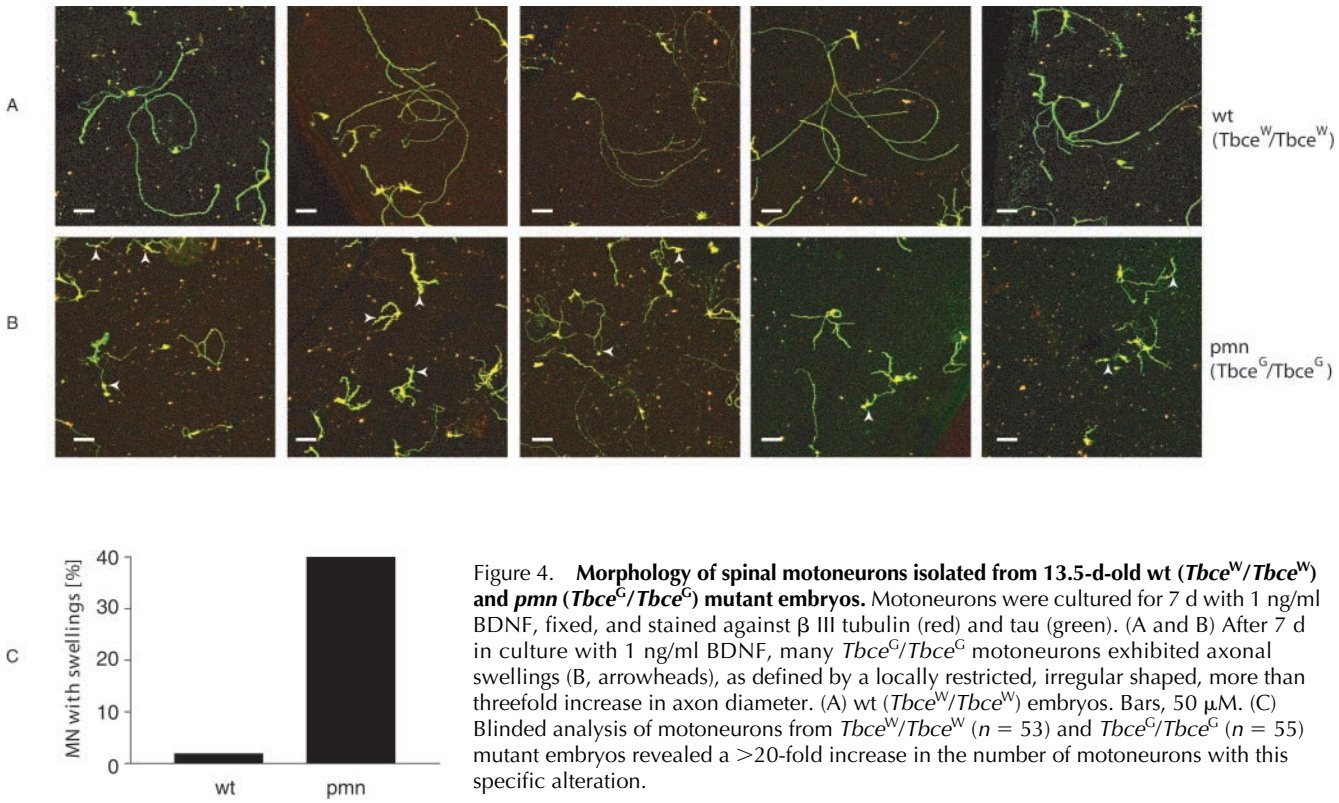

Figure 4. **Morphology of spinal motoneurons isolated from 13.5-d-old wt (*Tbce*^{W}/*Tbce*^{W}) and *pmn* (*Tbce*^{G}/*Tbce*^{G}) mutant embryos.** Motoneurons were cultured for 7 d with 1 ng/ml BDNF, fixed, and stained against β III tubulin (red) and tau (green). (A and B) After 7 d in culture with 1 ng/ml BDNF, many *Tbce*^{G}/*Tbce*^{G} motoneurons exhibited axonal swellings (B, arrowheads), as defined by a locally restricted, irregular shaped, more than threefold increase in axon diameter. (A) wt (*Tbce*^{W}/*Tbce*^{W}) embryos. Bars, 50 μM. (C) Blinded analysis of motoneurons from *Tbce*^{W}/*Tbce*^{W} (n = 53) and *Tbce*^{G}/*Tbce*^{G} (n = 55) mutant embryos revealed a >20-fold increase in the number of motoneurons with this specific alteration.

Moreover, *pmn* mutant motoneurons exhibited axonal swellings that were irregularly stained with antibodies against β III tubulin and tau, whereas axonal swellings were only observed in very few wt motoneurons (Fig. 4; Fig. 5, A–H). The percentage of motoneurons with prominent axonal swellings (more than threefold increase in axon diameter) was determined by a blinded observer, revealing a 20-fold increase in this specific pathological feature in *Tbce*^{G}/*Tbce*^{G} mutant motoneurons (Fig. 4 C). The growth cones that are mostly devoid of microtubular structures were morphologically indistinguishable in wt and *pmn* mutant motoneurons (Fig. 5, I–L).

Survival of wt and *pmn* mutant motoneurons was not different (Fig. 3 C). This finding indicates that the mutation in the *Tbce* gene does not primarily affect motoneuron survival, but disrupts axon growth and integrity. These data are in agreement with previous observations that crossing of a *bcl-2* transgene into *pmn* mice prevented the death of the motoneuron cell bodies but had no detectable effect on axon degeneration, progressive muscle weakness, or time of death (Sagot et al., 1995b).

To test whether the selectivity of the disease process is caused by specific expression of *Tbce* in motoneurons, we determined levels for *Tbce* mRNA by semiquantitative RT-PCR in spinal cord, several brain regions, and other organs of 3-wk-old mice. This time point was chosen because it reflects the most active stage of the disease process in *pmn* mutant mice. *Tbce* seems ubiquitously expressed in the nervous system and other organs, with no selectivity for spinal cord (Fig. S2 A, available online at http://www.jcb.org/cgi/content/full/jcb.200208001/DC1). Similar observations were made when isolated embryonic motoneurons (E13.5) were compared with cortical neurons (E13.5) or neural stem cells derived from E11.5 mouse embryos (Fig. S2 B). Thus, the disease process is not caused by specific expression of *Tbce* in motoneurons, and the patho-mechanism underlying the motoneuron disease in *pmn* mutant mice apparently is caused by other means than specific *Tbce* gene expression. This finding resembles observations in other forms of motoneuron disease, such as familial ALS and SMA. Neither Cu/Zn superoxid dismutase nor Smn is specifically expressed in motoneurons; therefore, the selectivity of the disease process for motoneurons is still elusive.

We do not know yet how the Trp→Gly mutation at position 524 of the CofE protein interferes with its cellular function. This mutation could destabilize the protein or lead to either reduced or even enhanced chaperone activity, but it may also change its subcellular distribution or alter its interaction with other cellular binding partners. Dysregulation of CofE could interfere with tubulin assembly in several ways. Loss of the CofE homologue Alp21 in *S. pombe* leads to severe microtubule disintegration and reduced viability (Radcliffe et al., 1999). Genetic inactivation of *PFI*, the orthologue of the vertebrate *Tbce* in *Arabidopsis*, leads to defects in microtubule organization, mitotic division, and cytokinesis, but does not primarily interfere with cellular survival (Mayer et al., 1999; Steinborn et al., 2002).

Forced overexpression of CofE in Hela cells sequesters α-tubulin, thus inhibiting dimer formation with β-tubulin and destabilizing free α- and β-tubulin subunits (Bhamidipati et al., 2000). Moreover, CofE, together with other tubulin-specific cofactors, can act as GTPase, converting GTP-tubulin to GDP-tubulin. Thus, the capacity of polymerization into microtubules is lost (Tian et al., 1999) either by overexpression, altered protein interactions, or loss of CofE.

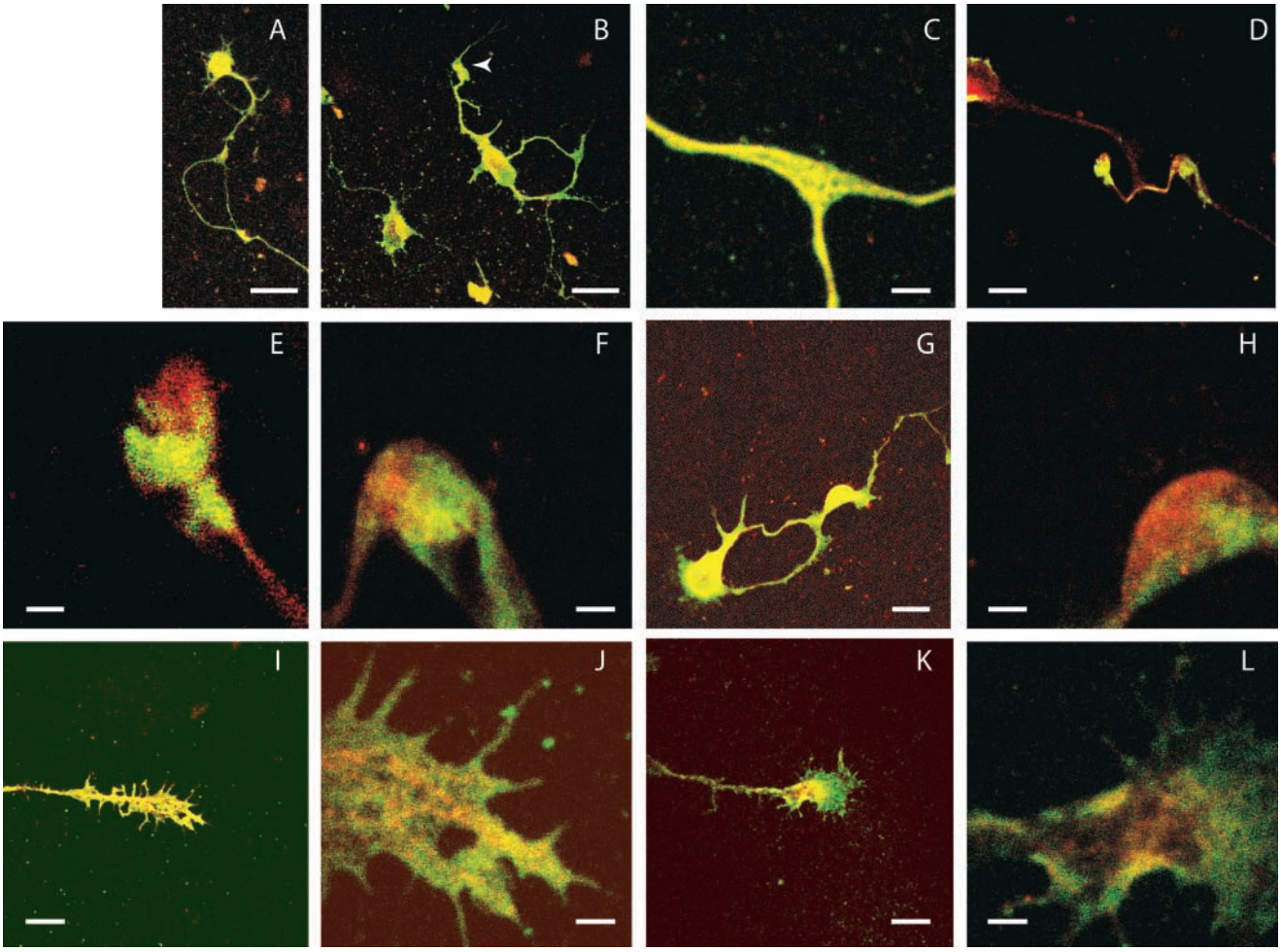

Figure 5. **Morphology of spinal motoneurons isolated from 13.5-d-old wt (*Tbce*^{W}/*Tbce*^{W}) and *pmn* mutant (*Tbce*^{G}/*Tbce*^{G}) embryos.** Motoneurons were cultured for 7 d with 1 ng/ml BDNF, fixed, and stained against β III tubulin (red) and tau (green). (A and B) Motoneurons derived from *pmn* mutant embryos (B) exhibit shorter axons compared with axons from control cells (A). In *pmn* mutant motoneurons axonal varicosities are detectable (B, arrowhead), which were rarely observed in wt motoneurons. (C–H) Whereas β III tubulin and tau immunoreactivity is regularly organized and evenly distributed in axonal branch points in motoneurons derived from wt embryos (C), immunoreactivity for β III tubulin and tau in *pmn* mutants (D–H) is irregularly distributed in aggregate-like structures, and both proteins do not colocalize. (I–L) In contrast, growth cones that are mostly devoid of microtubular structures are morphologically indistinguishable in wt (I and J) and *pmn* mutant motoneurons (K and L). Bars: (A and B) 25 μm; (C, E, F, H) 5 μm; (D and G) 25 μm; (J and L) 5 μm; (I and K) 25 μm.

Microtubules play an important role in axonal transport (Ishihara et al., 1999). The *pmn* mouse has been used in many studies as an animal model for motoneuron disease. Treatment of these mice with CNTF or other neurotrophic factors delays axon degeneration and motoneuron cell death (Sendtner et al., 1992; Haase et al., 1997). Neurotrophic factors enhance axonal transport both in retrograde (Sagot et al., 1998) and anterograde directions (Sahenk et al., 1994), and thus, at least in part, could functionally compensate for defects in microtubule structure in *pmn* mice (Sendtner et al., 1992; Sagot et al., 1995a).

The *pmn* mice appear healthy during embryonic development when axons grow out and make first contacts with skeletal muscle, resembling the clinical phenotype of human SMA. Thus, the function of CofE may become clinically relevant after birth. However, we observe a significant reduction in axonal growth in isolated embryonic *pmn* motoneurons. Nevertheless, the motoneurons still grow out axonal processes, suggesting that mechanisms exist that can at least partially compensate. This observation could reflect differential requirements of embryonic tubulin isoforms for CofE. It will be interesting to find out whether the class III β-tubulin isotype, which is highly expressed during development but not in the adult (Ferreira and Caceres, 1992), does not or to a lower degree depend on CofE.

Defects in microtubule function are associated with many forms of neurodegenerative disease. Deletion of kinesin, a microtubule-associated motor protein leads to severe motoneuron dysfunction in *Drosophila* (Hurd and Saxton, 1996). In human, Charcot Marie Tooth disease type 2A is caused by a mutation in the microtubule motor KIF1Bβ (Zhao et al., 2001). Recently, it was shown that overexpression of dynamitin leads to disturbed retrograde axonal transport and thus causes motoneuron disease in mice (LaMonte et al., 2002). The symptoms are similar to those observed in mice overexpressing neurofilament genes (Cote et al., 1993; Xu et al., 1993). Moreover, mutations in tau, another microtubule binding and stabilizing protein, are not only associated with

various forms of frontotemporal dementia (Garcia and Cleveland, 2001; Goedert and Spillantini, 2001) but also with the ALS/parkinsonism-dementia complex (Ishihara et al., 1999). Thus dysfunction of cellular mechanisms regulating tubulin assembly plays an essential role in motoneuron function and maintenance.

Materials and methods

Mouse strains

Two female AKR mice (Jackson ImmunoResearch Laboratories) and one male NMRI founder heterozygous for the *pmn* gene defect were bred and the F1 generation intercrossed for an F2 generation that could be used for genetic mapping of the *pmn* locus. The *pmn* mutation has been first detected at the Panum Institute (Kopenhagen, Denmark), where it spontaneously arose in a colony of NMRI outbred mice (Schmalbruch et al., 1991). This line was continuously backcrossed to NMRI (Jackson ImmunoResearch Laboratories) at our animal facility, and mice from this colony were used for confirmation of the *Tbce* gene mutation in *pmn* mice.

Genetic mapping of the *pmn* locus

Radioactive PCR with primers specific for the microsatellite markers was performed. Recombination events were investigated by size polymorphisms of the resulting fragments. A total of 229 *pmn/pmn* F2 offspring were genotyped with 29 microsatellite markers corresponding to a region spanning 31 cM from D13Mit1 to D13Mit10. 34 crossovers were identified, allowing us to map the *pmn* locus in a 2-cM region of chromosome 13 between D13Mit173 and D13Mit207.

Physical mapping of the *pmn* locus

All YAC clones were obtained from Research Genetics. The BAC clones were identified by screening of BAC mouse (release I and II) high-density filters with probes corresponding to the genes for *nidogen* and *Gli3*. All BAC clones were obtained from Genome Systems Inc., except BAC clone 369D23, which was supplied by Research Genetics. The physical map was created by testing all BACs and YACs for the presence of markers listed on the physical map and design of new sequence-tagged sites (STSs) generated by YAC and BAC clone end sequences. The novel STS sequences are listed in Table S2, available online at http://www.jcb.org/cgi/content/full/jcb.200208001/DC1.

Used databases

A Celera genomic scaffold covering ~2.19 Mb (nucleotides 9,285,719–11,297,173) located on mouse chromosome 13 was used to derive the genomic structure of 23 putative and previously identified transcriptional units.

Open reading frames were additionally confirmed using information deposited in public EST databases (www.ncbi.nlm.nih.gov/; Altschul et al., 1997). Only sequences of expressed genes were analyzed. Homology searches and sequence alignment were performed with BLAST (www.ncbi.nlm.nih.gov/; Altschul et al., 1997).

Sequence analysis of candidate genes

Total RNA from tissue of *pmn* and wt mice was prepared by the Trizol procedure (Invitrogen) and was reverse transcripted with oligo dT primers according to the manufacturer's instructions (Invitrogen). Primers used for PCR reactions and the specific PCR conditions are shown in Table S3, available online at http://www.jcb.org/cgi/content/full/jcb.200208001/DC1.

Double-stranded DNA was subjected to automated sequencing on an ABI 373 sequencer by dideoxy sequencing using a commercial standard DNA sequencing kit (ABI). Both strands were sequenced with respective primers. Resulting DNA sequences obtained from PCR products from *pmn* and NMRI wt mice were aligned to corresponding sequence information in databases in order to identify nucleotide variations.

Embryonic mouse motoneuron cultures

Spinal motoneurons from 13.5-d-old mouse embryos were isolated, enriched, and plated at a density of 3,000 cells/well on Greiner 4-well culture dishes as previously described (Wiese et al., 2001). Cells were grown in neurobasal medium, B27 supplement, 10% horse serum, 500 μM glutamax (Invitrogen), and 1 ng/ml BDNF. Medium was first replaced at day 1 and then every second day.

Surviving cells were counted under phase-contrast microscopy every second day. Initial counting of plated cells was done when all cells were attached to the culture dish at 4 h after isolation.

After 7 d in culture, motoneurons were fixed with 4% paraformaldehyde for 15 min at 4°C. The cells were washed with TBS (25 mM Tris/HCl, pH 7.4, 0.8% NaCl, 0.2% KCl). Nonspecific binding sites were blocked for 1 h with TBS containing 10% goat serum and 0.1% Tween-20. Cells were incubated for 24 h at 4°C with antibodies against β III tubulin (1:500; RDI) and tau (1:200; Sigma-Aldrich), and then washed three times with TBS. β III tubulin was visualized by goat anti–mouse Cy3 (5 μg/ml; Jackson ImmunoResearch Laboratories) and tau with goat anti–rabbit Cy2 (10 μg/ml; Jackson ImmunoResearch Laboratories) for 1 h. Cells were washed again three times with TBS, and then covered with Mowiol in 50% glycerol/PBS (vol/vol) and observed under a Leica confocal microscope (TCS; Leica). Controls were done in the absence of the first antibodies (not depicted).

Digital photographs of motoneurons were taken using a Leica confocal microscope. As previously described (Wiese et al., 1999), axons are at least three times longer than dendrites after 7 d in culture and thus can be distinguished. Axon length was determined by applying a morphometric system (ScionImage; Scion Corporation, Inc.). These analyses of mutant and wt motoneurons were performed blindly. The investigator did not know the genotype of the cultured cells. Values from independent experiments were pooled, and the results were expressed as the mean ± SEM. Statistical significance of differences were assessed by *t* test using the GraphPad Prism software.

Neural stem cells

Cultures of neural stem cell neurospheres from forebrain of embryonic day 11.5 mice were prepared and transferred to 100 μl HBSS. After treatment with trypsin (0.05%, 10 min; Worthington), cell suspensions were generated by trituration. Trypsin was inactivated with trypsin inhibitor from egg yolk sack (0.05%; Sigma-Aldrich) and the cells plated on 75-ml culture dishes (Greiner) in 5 ml neurobasal medium containing 500 μM glutamax, B27 supplement, and bFGF and EGF (Cell Concepts) at final concentrations of 10 ng/ml each. Medium was changed every second day. Cells from the supernatant were centrifuged at 400 *g*, triturated, and cultured in fresh medium. Cells were passaged at least six times to enrich neurospheres. These neurospheres were centrifuged and RNA was isolated.

Accession nos.

The GenBank/EMBL/DDBJ accession numbers for *Mus musculus* are as follows: NM031999 (*Tm7sf1*), NM 010917 (*Nid*), NM 010748 (*Lyst*), NM 010317 (*Gng4*), NM 010282 (*Ggps1*), AK018194 (*Rbp1-like*), AK002753 (*Mrpl*), NM 008944 (*Psma2*), and X95255 (*Gli3*). The following accession numbers are for *Homo sapiens*: NM 003193 (*TBCE*), NM 003272 (*TM7SF1*), NM 000081 (*CHS1*), 004485 (*GNG4*), NM 004837 (*GGPS1*), NM 016374 (*RBP1-like*), XM 045232 (*LOC94980*), NM 031903 (*MRPL32*), NM 002787 (*PSMA2*), NM 024054 (*MGC2821*), and BC021686 (*ELF-1α*). The accession number for *Tbce* is AV605313 for *Bos taurus*, BI314293 for *Xenopus laevis*, AF486851 for *A. thaliana*, and NP 501395 for *C. elegans*. The accession numbers from OMIM are as follows: 25330 (*SMA*), 604320 (*SMARD1*), 205100 (*ALS2*), and 118210 (Charcot Marie Tooth disease type 2A).

Online supplemental material

Figs. S1 and S2 and Tables S1, S2, and S3 are available online at http://www.jcb.org/cgi/content/full/jcb.200208001/DC1. Fig. S1 shows the *pmn* candidate region. Fig. S2 shows the expression profile of *Tbce* mRNA in neuronal and nonneuronal tissue. Table S1 shows the transcript map of the *pmn* region, including the syteny region of the human genome. Table S2 shows the novel STSs isolated from the *pmn* candidate region. Table S3 shows a list of primers used for PCR reactions.

We thank B. Holtmann for mouse husbandry and K. Grohmann for many helpful discussions. We also thank B. Christ, K. Blecharz, and C. Schneider for excellent technical assistance.

This work was supported by the Deutsche Forschungsgemeinschaft, SFB 581, TP B1, and B4, and by the Hermann and Lilly Schilling Stiftung. Part of these data was generated using the Celera Discovery System and Celera Genomics' associated databases.

Submitted: 1 August 2002
Revised: 17 September 2002
Accepted: 3 October 2002

References

Altschul, S.F., T.L. Madden, A.A. Schaffer, J. Zhang, Z. Zhang, W. Miller, and D.J. Lipman. 1997. Gapped BLAST and PSI-BLAST: a new generation of protein database search programs. *Nucleic Acids Res.* 25:3389–3402.

Bhamidipati, A., S.A. Lewis, and N.J. Cowan. 2000. ADP ribosylation factor-like protein 2 (Arl2) regulates the interaction of tubulin-folding cofactor D with native tubulin. *J. Cell Biol.* 149:1087–1096.

Cote, F., J.F. Collard, and J.P. Julien. 1993. Progressive neuronopathy in transgenic mice expressing the human neurofilament heavy gene: a mouse model of amyotrophic lateral sclerosis. *Cell.* 73:35–46.

Ferreira, A., and A. Caceres. 1992. Expression of the class III β-tubulin isotype in developing neurons in culture. *J. Neurosci. Res.* 32:516–529.

Garcia, M.L., and D.W. Cleveland. 2001. Going new places using an old MAP: tau, microtubules and human neurodegenerative disease. *Curr. Opin. Cell Biol.* 13:41–48.

Goedert, M., and M.G. Spillantini. 2001. Tau gene mutations and neurodegeneration. *Biochem. Soc. Symp.* 59–71.

Grohmann, K., M. Schuelke, A. Diers, K. Hoffmann, B. Lucke, C. Adams, E. Bertini, H. Leonhardt-Horti, F. Muntoni, R. Ouvrier, et al. 2001. Mutations in the gene encoding immunoglobulin μ-binding protein 2 cause spinal muscular atrophy with respiratory distress type 1. *Nat. Genet.* 29:75–77.

Haase, G., P. Kennel, B. Pettmann, E. Vigne, S. Akli, F. Revah, H. Schmalbruch, and A. Kahn. 1997. Gene therapy of murine motor neuron disease using adenoviral vectors for neurotrophic factors. *Nat. Med.* 3:429–436.

Hadano, S., C.K. Hand, H. Osuga, Y. Yanagisawa, A. Otomo, R.S. Devon, N. Miyamoto, J. Showguchi-Miyata, Y. Okada, R. Singaraja, et al. 2001. A gene encoding a putative GTPase regulator is mutated in familial amyotrophic lateral sclerosis 2. *Nat. Genet.* 29:166–173.

Hartl, F.U. 1996. Molecular chaperones in cellular protein folding. *Nature.* 381: 571–579.

Hoyt, M.A., J.P. Macke, B.T. Roberts, and J.R. Geiser. 1997. *Saccharomyces cerevisiae* PAC2 functions with CIN1, 2 and 4 in a pathway leading to normal microtubule stability. *Genetics.* 146:849–857.

Hurd, D.D., and W.M. Saxton. 1996. Kinesin mutations cause motor neuron disease phenotypes by disrupting fast axonal transport in *Drosophila*. *Genetics.* 144:1075–1085.

Ishihara, T., M. Hong, B. Zhang, Y. Nakagawa, M.K. Lee, J.Q. Trojanowski, and V.M. Lee. 1999. Age-dependent emergence and progression of a tauopathy in transgenic mice overexpressing the shortest human tau isoform. *Neuron.* 24:751–762.

LaMonte, B.H., K.E. Wallace, B.A. Holloway, S.S. Shelly, J. Ascano, M. Tokito, T. Van Winkle, D.S. Howland, and E.L. Holzbaur. 2002. Disruption of dynein/dynactin inhibits axonal transport in motor neurons causing late-onset progressive degeneration. *Neuron.* 34:715–727.

Lefebvre, S., L. Burglen, S. Reboullet, O. Clermont, P. Burlet, L. Viollet, B. Benichou, C. Cruaud, P. Millasseau, and M. Zeviani. 1995. Identification and characterization of a spinal muscular atrophy-determining gene. *Cell.* 80: 155–165.

Martin, N., J. Jaubert, P. Glaser, M. Szatanik, and J.L. Guenet. 2001. Genetic and physical delineation of the region overlapping the progressive motor neuropathy (pmn) locus on mouse chromosome 13. *Genomics.* 75:9–16.

Mayer, U., U. Herzog, F. Berger, D. Inze, and G. Jürgens. 1999. Mutations in the pilz group genes disrupt the microtubule cytoskeleton and uncouple cell cycle progression from cell division in *Arabidopsis* embryo and endosperm. *Eur. J. Cell Biol.* 78:100–108.

Radcliffe, P.A., D. Hirata, L. Vardy, and T. Toda. 1999. Functional dissection and hierarchy of tubulin-folding cofactor homologues in fission yeast. *Mol. Biol. Cell.* 10:2987–3001.

Radcliffe, P.A., M.A. Garcia, and T. Toda. 2000. The cofactor-dependent pathways for α- and β-tubulins in microtubule biogenesis are functionally different in fission yeast. *Genetics.* 156:93–103.

Sagot, Y., S.A. Tan, E. Baetge, H. Schmalbruch, A.C. Kato, and P. Aebischer. 1995a. Polymer encapsulated cell lines genetically engineered to release ciliary neurotrophic factor can slow down progressive motor neuronopathy in the mouse. *Europ. J. Neurosci.* 7:1313–1322.

Sagot, Y., M. Dubois-Dauphin, S.A. Tan, F. de Bilbao, P. Aebischer, J.C. Martinou, and A.C. Kato. 1995b. Bcl-2 overexpression prevents motoneuron cell body loss but not axonal degeneration in a mouse model of a neurodegenerative disease. *J. Neurosci.* 15:7727–7733.

Sagot, Y., T. Rosse, R. Vejsada, D. Perrelet, and A.C. Kato. 1998. Differential effects of neurotrophic factors on motoneuron retrograde labeling in a murine model of motoneuron disease. *J. Neurosci.* 18:1132–1141.

Sahenk, Z., J. Seharaseyon, and J.R. Mendell. 1994. CNTF potentiates peripheral nerve regeneration. *Brain Res.* 655:246–250.

Schmalbruch, H., H.J.S. Jensen, M. Bjaerg, Z. Kamieniecka, and L. Kurland. 1991. A new mouse mutant with progressive motor neuronopathy. *J. Neuropathol. Exp. Neurol.* 50:192–204.

Sendtner, M., H. Schmalbruch, K.A. Stockli, P. Carroll, G.W. Kreutzberg, and H. Thoenen. 1992. Ciliary neurotrophic factor prevents degeneration of motor neurons in mouse mutant progressive motor neuronopathy. *Nature.* 358: 502–504.

Steinborn, K., C. Maulbetsch, B. Priester, S. Trautmann, T. Pacher, B. Geiges, F. Küttner, L. Lepiniec, Y.-D. Stierhof, H. Schwarz, et al. 2002. The *Arabidopsis* PILZ group genes encode tubulin-folding cofactor orthologs required for cell division but not cell growth. *Genes Dev.* 16:959–971.

Tian, G., Y. Huang, H. Rommelaere, J. Vandekerckhove, C. Ampe, and N.J. Cowan. 1996. Pathway leading to correctly folded β-tubulin. *Cell.* 86:287–296.

Tian, G., S.A. Lewis, B. Feierbach, T. Stearns, H. Rommelaere, C. Ampe, and N.J. Cowan. 1997. Tubulin subunits exist in an activated conformational state generated and maintained by protein cofactors. *J. Cell Biol.* 138:821–832.

Tian, G., A. Bhamidipati, N.J. Cowan, and S.A. Lewis. 1999. Tubulin folding cofactors as GTPase-activating proteins. GTP hydrolysis and the assembly of the α/β-tubulin heterodimer. *J. Biol. Chem.* 274:24054–24058.

Wiese, S., F. Metzger, B. Holtmann, and M. Sendtner. 1999. The role of $p75^{NTR}$ in modulating neurotrophin survival effects in developing motoneurons. *Eur. J. Neurosci.* 11:1668–1676.

Wiese, S., G. Pei, C. Karch, J. Troppmair, B. Holtmann, U.R. Rapp, and M. Sendtner. 2001. Specific function of B-raf in mediating survival of embryonic motoneurons and sensory neurons. *Nat. Neurosci.* 4:137–142.

Xu, Z., L.C. Cork, J.W. Griffin, and D.W. Cleveland. 1993. Increased expression of neurofilament subunit NF-L produces morphological alterations that resemble the pathology of human motor neuron disease. *Cell.* 73:23–33.

Yang, Y., A. Hentati, H.X. Deng, O. Dabbagh, T. Sasaki, M. Hirano, W.Y. Hung, K. Ouahchi, J. Yan, A.C. Azim, et al. 2001. The gene encoding alsin, a protein with three guanine-nucleotide exchange factor domains, is mutated in a form of recessive amyotrophic lateral sclerosis. *Nat. Genet.* 29:160–165.

Zhao, C., J. Takita, Y. Tanaka, M. Setou, T. Nakagawa, S. Takeda, H.W. Yang, S. Terada, T. Nakata, Y. Takei, et al. 2001. Charcot-Marie-Tooth disease type 2A caused by mutation in a microtubule motor KIF1Bβ. *Cell.* 105:587–597.